Project 4 FYS4150

Kjetil Karlsen

November 19, 2017

Abstract

In this report we have run simulations of a simplified 2 dimensional Ising model using Monte Carlo methods and the Metropolis algorithm. Analytical values for the 2×2 system was calculated, and the mean magnetization, mean energy, heat capacity and susceptibility of lattices up to 100×100 was estimated. In addition, properties of second order phase transitions was investigated and the critical temperature of an infinite lattice was calculated to be $2.2777 \frac{k_B T}{J}$. The systems showed different behaviour at different temperatures, the mean values fluctuating more around the equilibrium at higher temperatures. At the critical temperature, the mean magnetization went to zero.

Throughout the project I have collaborated with Vilde Mari Johansen in developing the code and figures. This can be found at Github.

Contents

1 Introduction

Monte Carlo methods are widely used in both scientific and economic applications. One application is to study the Ising model, where the energy is decided by the configuration of the spins in a lattice. The aim of this project is to simulate a magnetic solid through the Ising model, investigating heat capacity, magnetization, susceptibility and critical temperatures at phase transitions.

This report starts by the describing simplified physics which describes the properties of a Ising solid and Boltzmann statistics. Systems of lattice sizes varying from 2×2 to 100×100 will be investigated, as well as the properties at the phase transition. The results of benchmark and stability of the algorithm will be discussed.

2 Theory

The theory and method sections are based on chapter 12 and 13 in Jensen, [1].

2.1 The Ising model

The Ising model is a model used to simulate magnetic phase transitions of solids. In this project a somewhat simplified version of the model will be used, assuming no external magnetic field and a finite, 2 dimentional system. It is also assumed that the each spin can only take the values $s = \pm1$. In this model only the nearest neighbours affect each other, excluding long range effects. The energy in a system of a total of N spins is then defined as

$$E = -J \sum_{\langle jk \rangle}^{N} s_k s_l \tag{1}$$

with J being a coupling constant and $\langle jk \rangle$ indicating that the sum is over the nearest neighbours only. The useful quantity Energy per spin is defined as $E_{spin} = \frac{E}{N}$.

2.1.1 Statistical physics in the Ising model

The spins in the Ising model follows Boltzmann statistics, meaning that the probability of a state $|i\rangle$ is defined as

$$P(E_i) = \frac{e^{-E_i\beta}}{Z_\beta} \tag{2}$$

with the partition function $Z_\beta = \int dE\, e^{-E\beta}$ normalizes the expression and $\beta = (k_B T)^{-1}$. The partition function used in the project is discrete, $Z_\beta = \sum_i^N e^{-E_i\beta}$. As the temperature T increases, the probability of each state decreases, giving a broader distribution of probable states.

In order to characterize the system, the mean energy, mean magnetization and mean absolute magnetization are important. The macroscopic property of mean energy $\langle E \rangle$ is needed to define the heat

capacity C_V of the system, while the microscopic effect of mean magnetization and the magnetic moment leads to the susceptibility χ. These are defined below:

$$\langle E \rangle = \frac{1}{Z_\beta} \sum_i^N E_i P_\beta(E_i) \tag{3}$$

$$\langle M \rangle = \frac{1}{Z_\beta} \sum_i^N M_i P_\beta(E_i) \tag{4}$$

$$\langle |M| \rangle = \frac{1}{Z_\beta} \sum_i^N |M|_i P_\beta(E_i) \tag{5}$$

$$C_V = \frac{1}{k_B T^2} \left(\langle E^2 \rangle - \langle E \rangle^2 \right) \tag{6}$$

$$\chi = \frac{1}{k_B T} \left(\langle M^2 \rangle - \langle M \rangle^2 \right) \tag{7}$$

Heat capacity, how the energy of a given system changes with temperature, is also analytically defined as

$$C_V = \left(\frac{\partial E}{\partial T}) \right)_V \tag{8}$$

2.1.2 Periodic boundary conditions

At the boundaries of a finite spin matrix it is fewer nearest neighbours than in the bulk of the matrix. This is analogous to a surface of a material. By assuming periodic boundary conditions, the effects of the surface is neglected and easy to handle. For a 1 dimensional case with N spins, the neighbours of spin S_N is S_{N-1} and S_1.

2.2 Phase transitions

A phase transition happens when a thermodynamically stable state of a system changes abruptly as one or more thermodynamical variables describing the structure reaches a critical value. In addition to changing state, macroscopic properties of the system must change. Melting of a solid is a example of an everyday phase transition, depending on a critical pressure and a critical temperature. At a critical temperature (T_C) the Ising model undergoes a second order phase transition, affecting both the mean energy and magnetization.

A first order phase transition is a gradual change from a phase to another and have two phases that coexist at the critical point, for example the melting of ice. The long range ordering exist in each phase, which gives a relatively large correlation length. For a second order phase transition, in the Ising model caused by Boltzmann statistics , the correlation length spans the entire system at the critical point. This means that the two phases on either side of the critical point is the same.

For a finite lattice the correlation length, mean magnetization, susceptibility and heat capacity is described by the following equations near the critical temperature.

$$\chi(T) \simeq (T_C - T)^{-\alpha} \tag{9}$$

$$\xi(T) \simeq |T_C - T|^{-\nu} \tag{10}$$

$$C_V(T) \simeq |T_C - T|^{-\gamma} \tag{11}$$

$$\langle M \rangle \simeq |T - T_C|^{\beta} \tag{12}$$

$$\tag{13}$$

The critical exponents α, β, ν and γ are all positive. From equation 9-11 it is clear that χ, $\xi(T)$ and C_V diverges to infinity at $T = T_C$. As the correlation length spans the whole system, it is limited by the lattice size, L. The critical temperature is related to the finite scaling by equation 14

$$T_C(L) - T_C(L = \infty) = aL^{-1/\nu} \tag{14}$$

The analytical value of $T_C = kTC/J = 2/\ln\left(1 + \sqrt{2}\right) \approx 2.269$ was reported by Onsager [2]

2.3 Scaling

In this project there is only one expression that needs to be scaled, namely $e^{-\beta E}$. By introducing $T' = \frac{k_B T}{J}$ and $E' = JE_{kl}$, with $E_{kl} = \sum_{<k,l>} s_k s_l$ this expression can be written as $e^{-E'/T'}$.

2.4 Simple example of the Ising model

It is possible to model the 2×2 Ising model with periodic boundary conditions analytically. This specific system has $N = 2^{L^2} = 2^4 = 16$ different micro states.

Table 2.1: Overview of the degeneracy of the $L = 2$ system. See table 6.1 for all the different microstates

No spin up	Deg	Energy	Magnetization
0	1	-8J	-4
1	4	0	-2
2	4	0	0
2	2	8J	0
3	4	0	2
4	1	-8J	4

From table 2.1 it is possible to calculate the partition function of the system:

$$Z = \sum_i^M e^{-\beta E_i} = 2e^{-\beta 8J} + 2e^{\beta 8J} + 12 = 4\cosh(\beta 8J) + 12$$

The mean energy is given as a derivation by parts of $\ln Z$ with regards to β:

$$\langle E \rangle = -\left(\frac{\partial \ln Z}{\partial \beta}\right)_{V,N} = -\frac{\partial}{\partial \beta} \ln\left[4\cosh(8J\beta) + 12\right] = \frac{-8J\sinh(8J\beta)}{3\cosh(J\beta) + 4}$$

By investigating table 2.1, the mean magnetization $\langle M \rangle$ must be 0. However, that is not true for the mean absolute magnetization:

$$\langle |M| \rangle = \frac{1}{Z} \sum_i^M M_i e^{\beta E_i} = \frac{(8J)^2 \cosh(8J\beta)}{\cosh(8J\beta) + 3}$$

By using the same methods as above, the expressions for $\langle E^2 \rangle$ and $\langle M^2 \rangle$ is found to be:

$$\langle E^2 \rangle = \frac{8\left(e^{8J\beta} + 1\right)}{\cosh(8J\beta) + 3}$$

$$\langle M^2 \rangle = \frac{2\left(e^{8J\beta} + 2\right)}{\cosh(8J\beta) + 3}$$

Combining these gives the expressions for the heat capacity and susceptibility from equations 6 and 7.

$$C_V = k\beta^2 \left(\langle E^2 \rangle - \langle E \rangle^2 \right) = \frac{\beta(8J)^2}{T} \left(\frac{\cosh^2 x - \sinh^2 x + 3\cosh x}{(\cosh x + 3)^2} \right) = \frac{(8J)^2}{k_B T^2} \frac{3\cosh x}{(\cosh x + 3)^2}$$

with $x = 8J\beta$. Similary, χ is found to be

$$\chi = \beta \left(\langle M^2 \rangle - \langle M \rangle^2 \right) = \frac{8\beta\left(e^x + 1\right)}{\cosh x + 3}$$

The real usefulness of the $L = 2$ periodic system is that it describes all the nearest neighbour interactions, for any lattice size.

3 Method

We want to study the Ising model at equilibrium. However, the system has to start from a initial condition. Markov chains are useful for this.

OBS: Bruker forventing av abs(M) i susceptbilitet.

3.1 Markov chains

The idea behind the markov chains is to make a random movement with a given probability of actually making the move, describing the microscopic principle of Brownian motion. This is often done by an eigenvalue problem, using a stochastic matrix W with the probabilities of making a move. As the eigenvalue of a $L \times L$ stochastic matrix has L eigenvalues with $\lambda_1 = 1$, $\lambda_i < 1$, it will eventually converge towards a equilibrium eigenvector through the relation $w_N = W^n w_0$. The steady state is reached when $w_{i+1} = W w_i$. In real life, this corresponds for instance to a particle diffusing through a solid. This particle has at every given moment a specific energy and in order to diffuse it has to overcome an energy barrier. However, a markov chain needs to obey the principles of ergodicity and detailed balance.

3.2 Metropolis algorithm

The matrix W is often unknown and in the metropolis algorithm it is instead described by $W = AT$. The acceptance probability of the problem is handled by matrix A, while the physics of the problem is handled by matrix T, describing the likelihood of making a transition. The detailed balance guaranties that the most likely state is reached, ie. that the probability of state w_i to transit to state w_j is the same as back from w_j to w_i: $w_j T(j \to i) A(j \to i) = w_i T(i \to j) A(i \to j)$.

In this project, the probability of a certain state is $w_i = \frac{1}{Z_\beta} e^{-\beta E_i}$ and the physics of moving between w_i and w_j is the same, one gets the following relation:

$$w_j = \frac{A(i \to j)}{A(j \to i)} w_i = e^{-\beta \Delta E} w_i \tag{15}$$

A system developing like this, with $\Delta E = E_j - E_i$ will reach the most likely state eventually. However, a real system fluctuates around the equilibrium. In order to ensure this, it must be probable to reach a state with higher energy than the previous. For the algorithm used in this project, all situations where the energy got lower by making a random transition, $E_{i+1} < E_i \Rightarrow \frac{w_{i+1}}{w_i} \geq 1$ was accepted. But also some states with $\frac{w_{i+1}}{w_i} > 1$ was accepted by random acceptance. Another important feature of equation 15 is that there is no need to calculate the partition function, which for large systems would lead to numerical errors.

For each Monte Carlo cycle our algorithm tried L^2 transitions, accepting only those transitions that fulfilled the requirements set in the previous section. This was done in order to directly compare how different matrix sizes converged to an equilibrium as a function of Monte Carlo cycles. All values calculated in section 4 were also divided by the total number of spins in the matrix (L^2), so that all values could be compared regardless of matrix size.

3.3 Random numbers

An ideal random number generator is not deterministic and produces an infinite number of different random numbers. However, this is not the case for a real generator. Every computer generated pseudo random generator will reproduce the same set of random numbers after a given period, which should be as large as possible. This means that a deterministic computer cannot produce a true random number, but a good pseudo random number generator has a negligible correlation between the different numbers. In this project the Mersene Twister 19937 generator (64 bit) was used, which has a period of 2^{19937}.

3.4 Parallelizing and speed up

Parallel computing represents a big increase in speed of these simple Monte Carlo calculations. When computing in parallel, the same program runs on a multitude of threads, effectively doing several experiments at the same time. A computer with two CPU's will be able to run the two programs parallel, collecting the data in the end. For this project parallel computing was utilized to split up the number of Monte Carlo cycles by the number of available CPU's. Assuming that the number of Monte Carlo cycles the system need to reach equilibrium is negligible compared to the total Monte Carlo cycles in the experiment, this approach is reasonable. By running on computer with p CPU's, this should give a speedup, defined by $Speedup(code, sys, p) = T_1/T_p$ of approximately 0.5.

Another way to increase the speed of the algorithm is to precalculate the energy. As there are only 16 changes in energy by changing a single spin, discussed in section 2.4, it is possible to pre-calculate $e^{-\beta\Delta E}$. Not only does this save FLOPS, but calculating the exponent is costly procedure.

3.5 Unit tests

In the program located at the github adress, there is no unit tests. As the finial state is expected to fluctuate around the equilibrium after the equilibrium is reached, the unit tests would need to deal with this fluctuation. We found it simpler to do this visually. In addition we checked each new element of the code as we developed the algorithm, a good example would be that the random number generator returned what looked like truly random numbers on the interval we wanted.

A possible unit test would be to check that the case with $L = 2$ gave approximately the analytical results for the various expectation values. Another relevant unit test could be to check that flipping one spin actually reproduced the ΔE which was computed analytically.

4 Result

4.1 The L=2 case

As the Monte Carlo cycles increases, the mean energy in figure 4.1a stabilizes around the analytical value for $T = 1\frac{k_B T}{J}$, which is calculated from equation 3. After it reaches equilibrium around $0.25 \cdot 10^7$ MC cycles, it is however not constant and fluctuates. In addition it is not aligning perfectly with the analytical value, but it is accurate to the fourth digit. This can be seen from figure 4.1b.

Figure 4.2 shows the same trend for $\langle |M| \rangle$ and $\langle M \rangle$. Both measurements equilibrates in roughly the same amount of MC-cycles, but there is a significant difference in the behaviour after equilibrium is reached. $\langle M \rangle$ is fluctuating much more about the analytical value. All calculations in this subsection are at T = 1.0 $\frac{k_B T}{J}$.

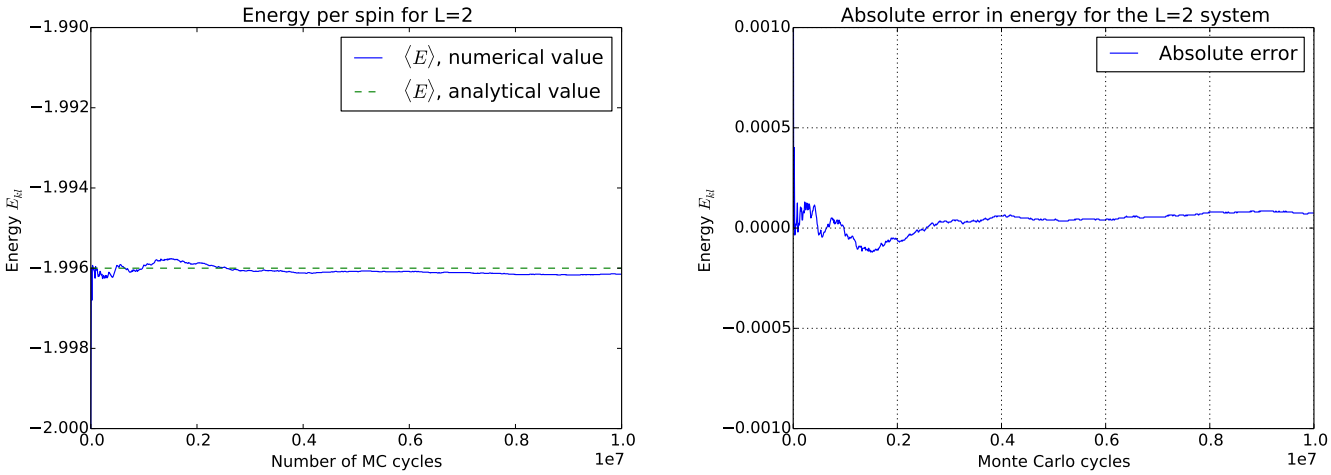

(a) Mean energy as a function of Monte Carlo cycles.

(b) Mean absolute error for the energy

Figure 4.1: Mean energy and mean absolute error of the energy at $T = 1\frac{k_B T}{J}$.

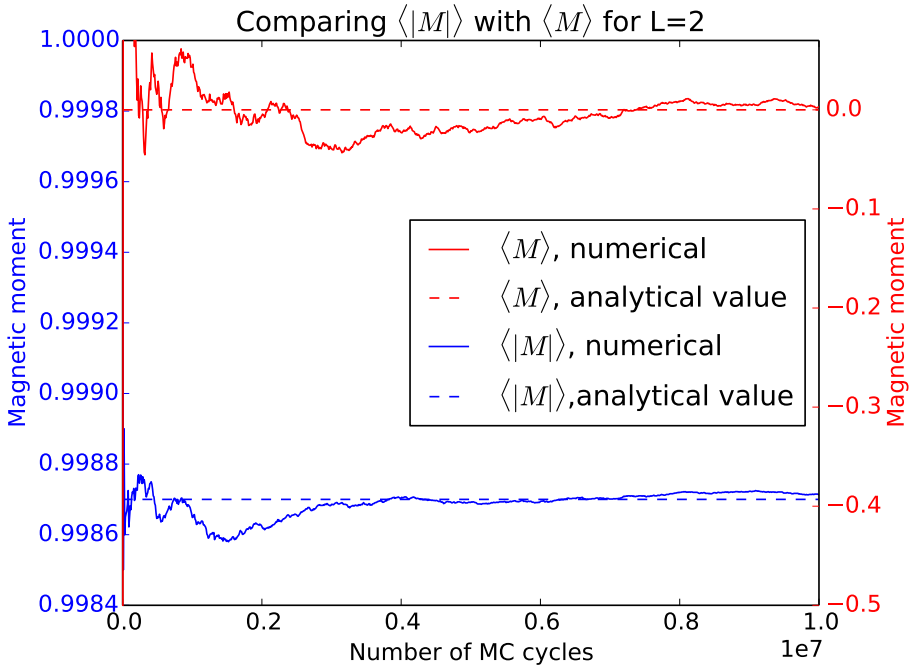

Figure 4.2: Comparison of the mean magnetization and the mean absolute magnetization.

Due to the smaller fluctuation of $\langle |M| \rangle$, the susceptibility for the system was calculated by

$$\chi = \frac{1}{k_B T} \left(\langle M^2 \rangle - \langle |M| \rangle^2 \right) \tag{16}$$

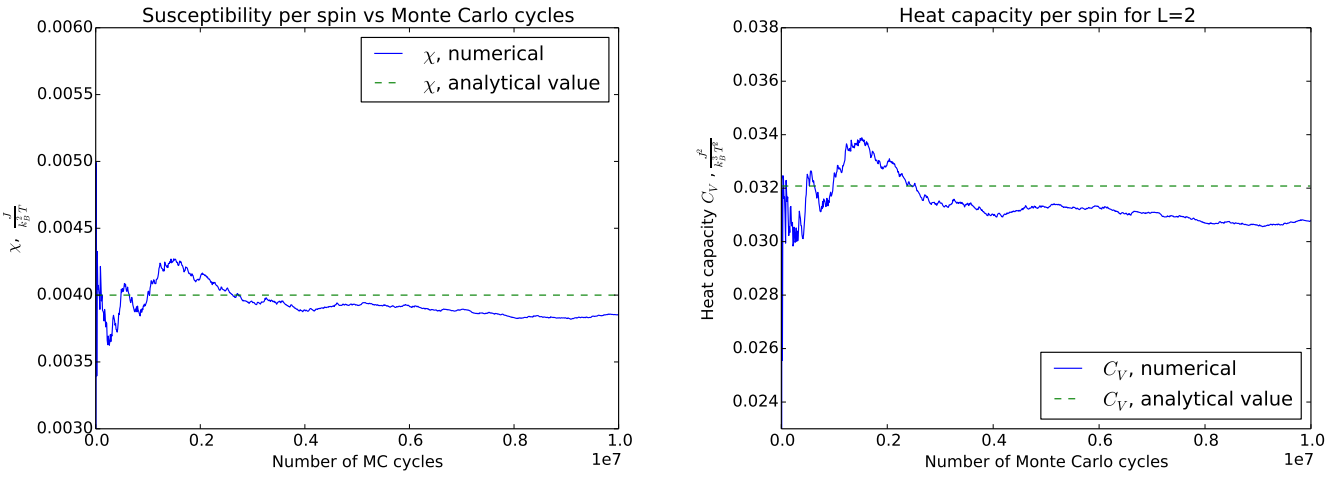

(a) (b)

Figure 4.3

4.2 The L=20 system

4.2.1 Initial ordering of the system and equilibrium time

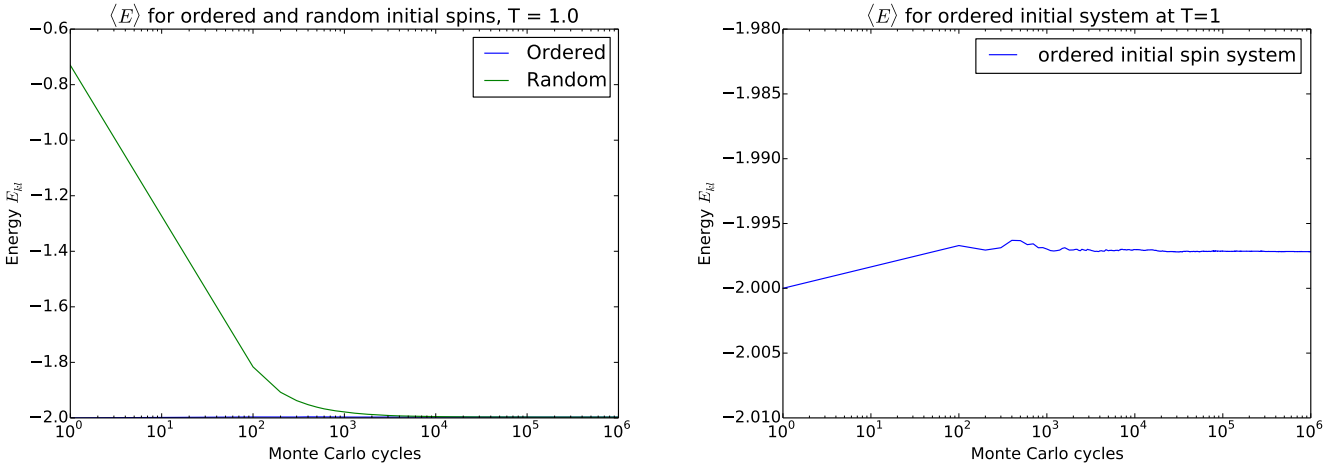

(a) Comparison of the mean energy with both ordered and random initial spin configuration.

(b) Closeup of the $\langle E \rangle$ for the ordered initial configuration

Figure 4.4: Comparison of the mean energy with both ordered and random initial spin configuration at T = 1 $\frac{k_B T}{J}$ on an logarithmic x axis.

Both the initial and the ordered initial matrix converges towards the same value after a significant number of Monte Carlo cycles. The ordered initial matrix started in the lowest possible energy state. From figure 4.4a, the random initial matrix seems to have an equilibration time of approximately 10^5 Monte Carlo cycles. As the ordered initial matrix changes a lot less, it is only possible to read

this information from figure 4.4b and this initial condition also seems to converge after 10^5 Monte Carlo cycles.

The behaviour in figure 4.5 is a bit more chaotic. The equilibrium value of $\langle E \rangle$ is higher than for T = 1, and change in value for the first 10^3 MC-cycles is large compared to figure 4.4a. However, after approximately 10^5 Monte Carlo cycles both the random and ordered initial matrix seems to converge to the same mean energy. In this intervall, between 10^5 and 10^6 MC-cycles the fluctuations in the mean energy is significantly smaller than between 10^3 and 10^5 cycles.

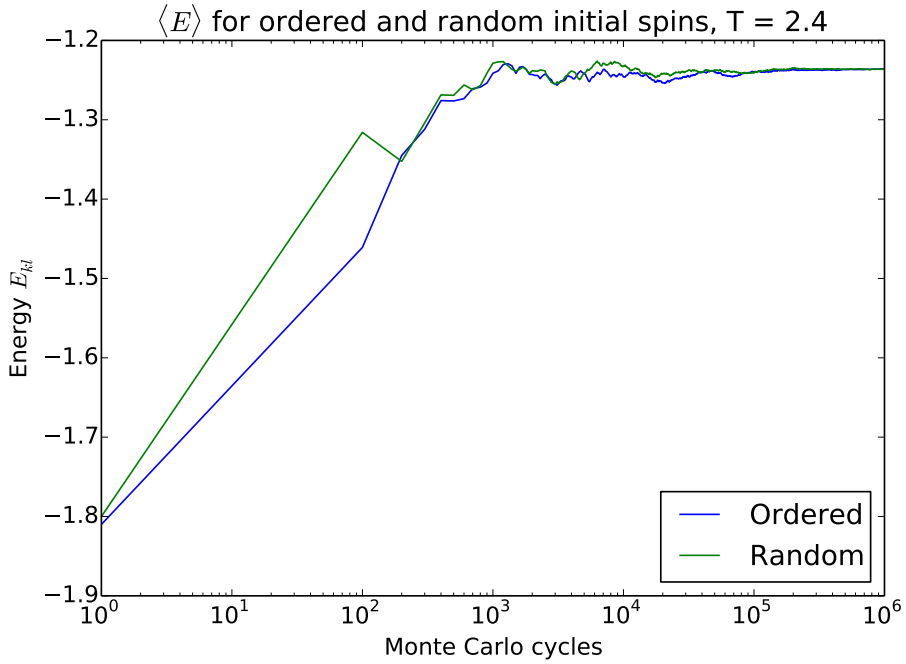

Figure 4.5: Comparison of the mean energy with both ordered and random initial spin configuration at T = 2.4 $\frac{k_B T}{J}$ on an logarithmic x-axis.

Figures 4.6 provides a closer look at the equilibrium behaviour of the L=20 system. The same trend shown in figure 4.4a and 4.5 for the behaviour of the system towards equilibrium is here seen around the equilibrium. For temperature T = 1 the fluctuations are small compared to the fluctuations for T =2.4. In addition the mean magnetization and energy is fully converged around $0.2 \cdot 10^6$, which is slower than the equilibration time of $0.1 \cdot 10^6$ for T =1. Both figures 4.6a and 4.6b show that the energy and magnetization is strongly correlated, converging at the approximately the same time.

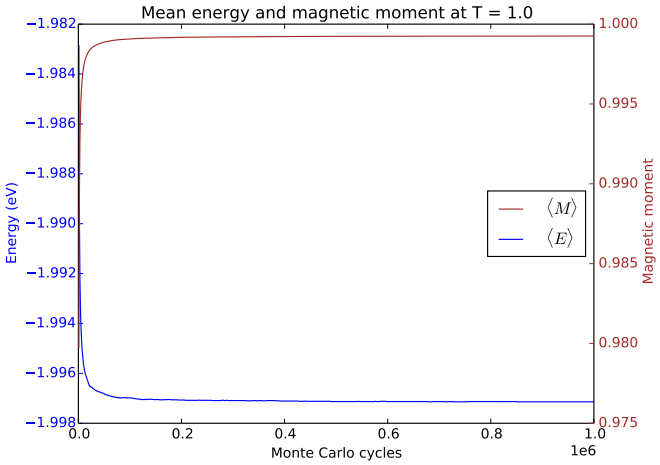

(a) Mean magnetization and energy at T = 1

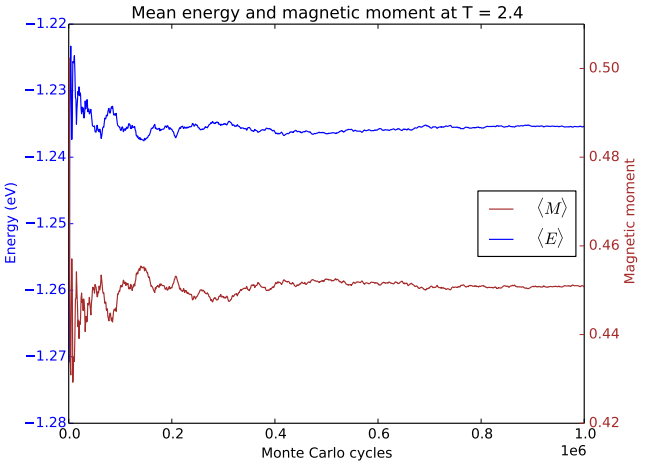

(b) Mean magnetization and energy at T = 2.4

Figure 4.6: Mean magnetization and energy on a linear x-scale for the randomly initialized L=20 system at T = 1 and T = 2.4

Figure 4.7b show how many attempts at changing a spin in the matrix is accepted at equilibrium. Both temperatures show a that fewer than 0.5% is accepted. Figure 4.7b shows the total accepted configurations, with the temperature $T = 2.4$ having accepted more configurations. Even though the probability of accepting a change of spin is low, both temperatures accumulate more configurations. However, the gradient of increase is highest between around $0 \cdot 10^6$, meaning the range $0 - 10^5$ Monte Carlo cycles.

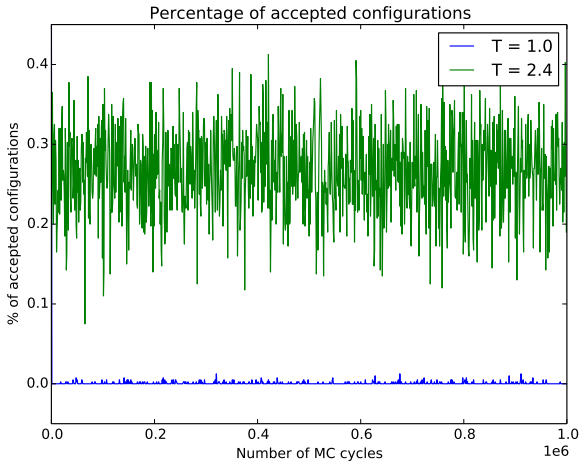

(a)

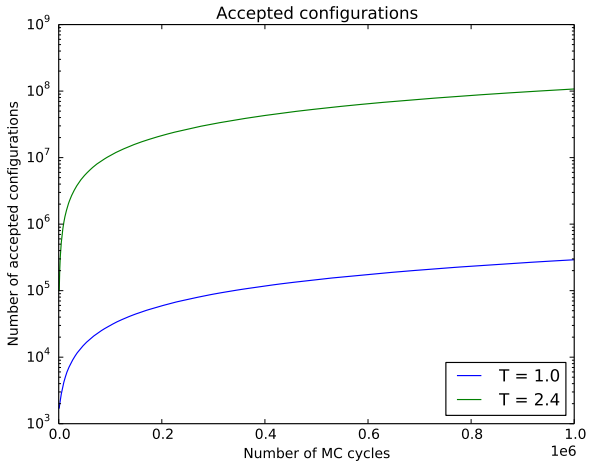

(b)

Figure 4.7

4.2.2 Probability distrubition for the L=20 system

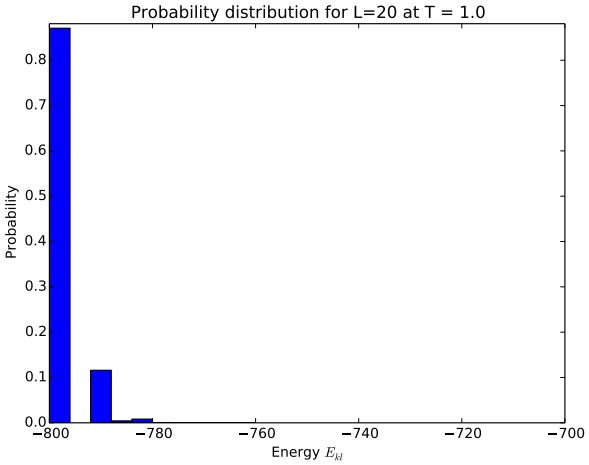

(a) Distribution of energies after equilibrium for T = 1

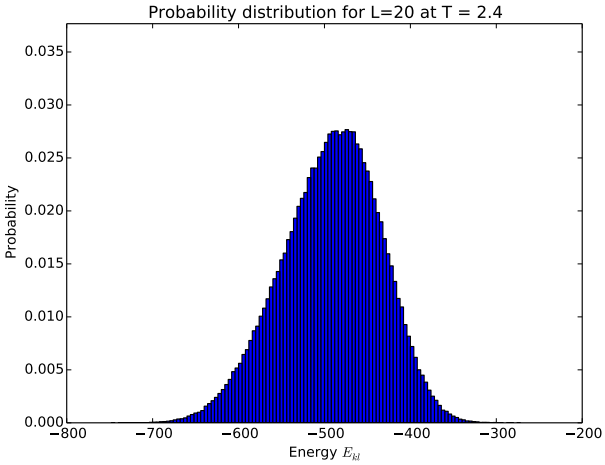

(b) Distribution of energies after equilibrium for T = 2.4

Figure 4.8: Normalized distribution of energies at equilibrium, after the $5 \cdot 10^5$ MC-cycles

Figure 4.8b shows a distribution not unlike a Gaussian distribution, while 4.8a has a high probability for the lowest energies and a probability that goes towards zero for higher energies. This is coherent with the data in table 4.1, where the higher temperature $T = 2.4$ has both significantly higher standard deviation and variance than the $T = 1$ case.

Table 4.1: Table of the standard deviation and expectation value of energy for the L = 20 system

Temperature ($\frac{k_B T}{J}$)	σ_E^2	σ_E
2.4	3213.71	56.69
1	11.36	3.37

4.3 Phase transition and Critical temperature

In figures 4.9 and 4.10, both the susceptibility and heat capacity peaks around a temperature of 2.3 for all grid sizes. The critical temperatures is stated in table 4.2. Around the critical temperature, the interval between the temperatures is $dT = 0.01$, while between $T = 2.1 \rightarrow 2.2$ and $T = 2.4 \rightarrow 2.6$ it is approximately $dT = 0.05$.

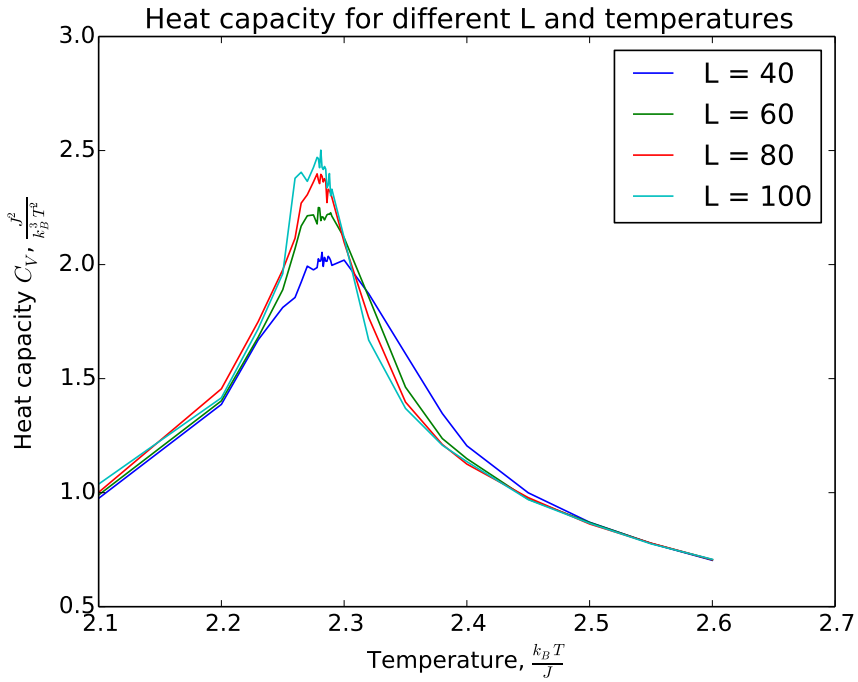

Figure 4.9: Susceptibility as a function of temperature and matrix size

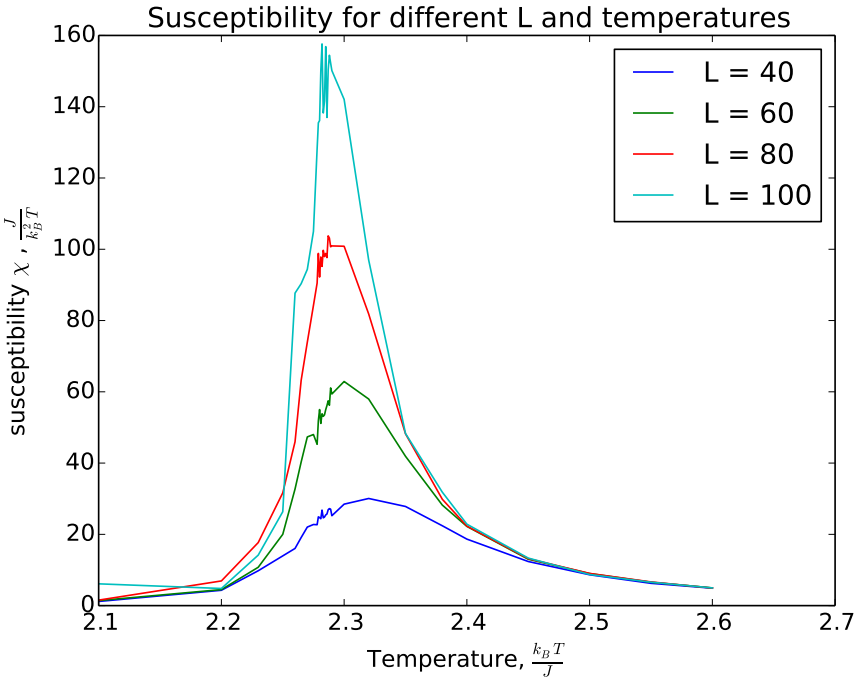

Figure 4.10: Heat capacity as a function of temperature and matrix size

At the critical temperature, the energies of the different systems is no longer the same, see figure 4.11a. But they are following the same trend, increasing mean energy as the temperature increases. However, the magnetization drops suddenly towards a $\langle M \rangle = 0$ at the critical temperature. The trend is also that larger lattices goes faster towards $\langle M \rangle = 0$ than the smaller lattices.

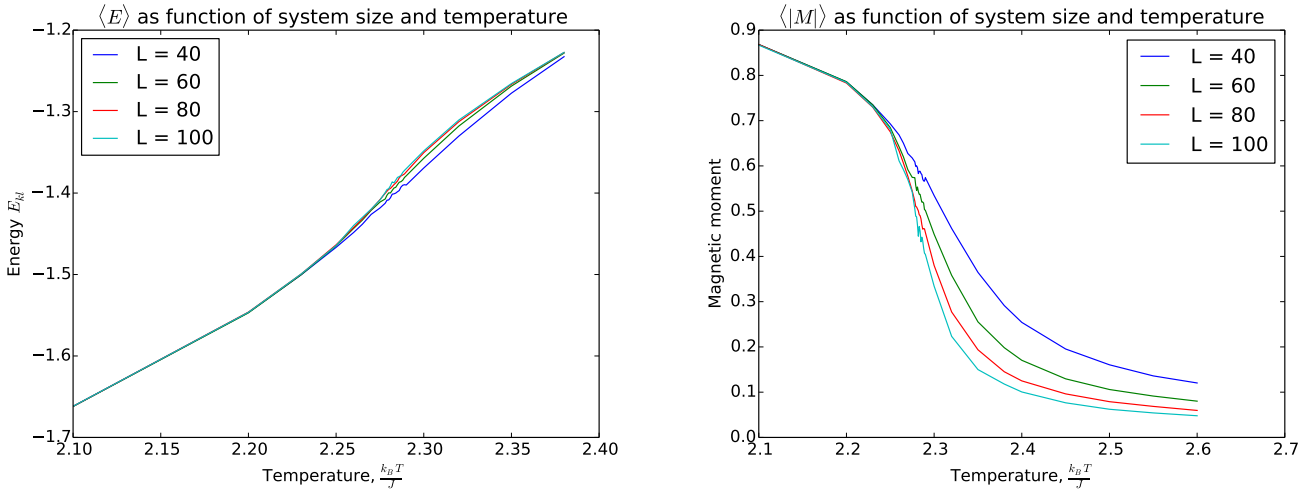

(a) Mean energy as a function of temperature and matrix size

(b) Mean magnetization as a function of temperature and matrix size

Figure 4.11: Mean magnetization and energy as a function of temperature and matrix size

For the critical temperatures there is no clear trend, see table 4.2. In order to find T_C for a system with $L = \infty$, the data from table 4.2 was plotted against the inverse lattice size. This gave a $T_C(L = \infty) = T_C(1/L = 0) \simeq 2.2777 \frac{k_B T}{J}$.

Table 4.2: text

L	T_C
40	2.282
60	2.279
80	2.278
100	2.281

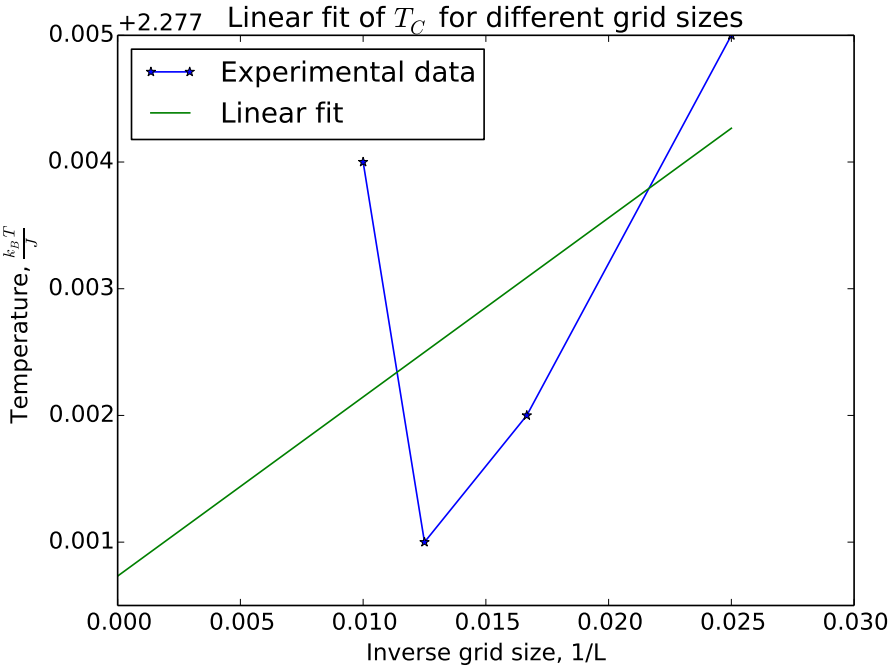

Figure 4.12: linear fit of the critical temperatures as a function of inverse grid size

4.4 Speedup

From table 4.3 it is clear that computing in parallel gives a speedup. The calculations were carried out for the case of L = 60, two temperatures and a total of 10^6 MC cycles on a computer with a 2 core i5 processor. This yields a speedup of $\frac{T_1}{T_2}$ = 0.598. Because of factors like the MPI_reduce function, the speedup is not the ideal 0.5.

Table 4.3: Overview of the time spent computing the L=60 system with two temperatures.

Number of cores:	CPU time [s]:
1	513.069
2	306.975

5 Discussion

5.1 The L=2 case

The mean magnetic moment is fluctuating more than the mean absolute magnetic moment, see figure 4.2. A small system is strongly dependent on the periodic boundary conditions, meaning that for the L=2 system, three out of four spins determine each E_i, linking them strongly together. This again means that if one spin changes, this very quickly have consequences for all the other spins. As this effect is expected to be lower at larger lattices, the smear out results of $\langle |M| \rangle$ is prefered to $\langle M \rangle$ for calculating the magnetic susceptibility.

Figure 4.1a shows that the $\langle E \rangle$ stabilizes at a lower value than the analytically calculated value, an effect also seen by the behaviour of χ and C_V. The plots show the clear trend of the statistical development of the system to the most likely state, but it also shows that Monte Carlo methods will not give exact answers. However the error is in the fourth digit and give a good approximation of the analytical value. Due to the random acceptance of less likely states, fluctuation is also seen.

It is also clear that the microscopic property of $\langle M \rangle$ is correlated to $\langle E \rangle$, as expected from equation 1.

5.2 The L=20 system

From the plots of the mean magnetization and energy for different temperatures, figures 4.6, it is clear that the equilibration time is not identical for different temperatures. This is probably partly due to the fact that higher temperatures fluctuates more, both while converging towards equilibrium and at the equilibrium. In order to be safe, a equilibration time of $2 \cdot 10^5$, corresponding to that of the highest temperature, and T = 2.4. This time corresponds to $0.2 \cdot 10^6$ Monte Carlo cycles, an important number when computing in parallel the way we chose to. As each thread calculated 10^6 Monte Carlo cycles, the equilibration time corresponds to only 20% of the total amount of calculations. This means that the majority of each thread is at equilibrium when collecting the different parallel simulations.

As the temperature increases, the likelihood that the system will change energy at equilibrium increases. This is due to inherent properties of the Boltzmann distribution. As the temperature increases, the difference between $e^{-\beta E_i}$ and $e^{-\beta E_j}$ decreases, resulting in higher variance for high temperatures. In real life, this corresponds to that the average thermal energy of each particle increases. Figure 4.6b shows this behaviour as greater fluctuations in both $\langle E \rangle$, and $\langle M \rangle$ at higher temperatures.

5.3 Phase transition, Critical temperature and benchmarks

When a phase transition occur, the properties of a system changes abruptly. By studying equation 8 and figure 4.11a, the gradient increases T = 2.3. In figure 4.9 this is mapped as a peak. The temperature corresponding to the top of the peak is the critical temperature, where the properties changes quickest. Figure 4.9 indicates that the larger L, the more abruptly the system changes properties. For smaller lattices, the change is more gradual. As the heat capacity diverges for an infinite lattice, sharper peaks for higher lattice sizes is expected. The same applies for χ.

By increasing the temperature resolution around T_C in the experiment, the hope was to gain a more precise value for $T_C(L = \infty)$. However, the results show a fluctuation in this region, disrupting the expected trend for $T_C(L)$. Figures 4.9 and 4.10 shows that for L=80 and L=100, the maximum is at a different temperature than what would be expected by a symmetric peak.

This fluctuation is not only located around T_C, but is expected to occur at all temperatures, as long as the temperature resolution is big enough. The temperature step, dT, is relatively large on the interval $T = 2.1 - 2.2$ and $T = 2.4 - 2.6$ and the values of C_V and χ changes significantly, the fluctuating effect is negligible.

Both the mean energy and magnetization fluctuates at random around equilibrium. The scale of this fluctuation is related to the temperature, as figure 4.8 indicates. When running 10^6 Monte Carlo cycles and collecting only C_V and χ at the last MC-cycle, no two runs at the same temperature would yield the same results.

Figure 4.12 and table 4.2 is affected by this, failing to illustrate the expected trend of lower T_C for larger lattices.

The CPU-timing shows a clear speedup, but not as large as expected. This is most likely caused by factors like the MPI_reduce function. This function performs a lot more calculations with two threads as with only one thread.

6 Conclusion

The metropolis algorithm for determining the probability of a jump in a Monte Carlo cycle is a descent method. This report shows that it is not completely accurate, but the simplicity and speed it offers for complicated systems makes up for that. Together with parallel computing, the overall time of the program was manageable. As the algorithm also allows for spin transitions that increase the overall energy, thus fluctuating around equilibrium, there is a limit to the precision of the produced data.

With increasing temperature, thus increasing the average thermal energy, resulted in increased mean energy and decrease of mean magnetization. This also affected the probability distribution of the different energies available at equilibrium, from a step function at T = 1 to a distribution looking like the normal probability distribution. In addition, the Ising model shows a clear phase transition around a critical temperature, which is dependent on the size of the spin matrix. This affected the total magnetisation, by suddenly dropping towards 0 at T_C.

When calculating the behaviour around the critical temperature, the highest temperature resolution should be used over the entire temperature range. It would also be a good addition to include larger spin matrices, as the estimate of the $T_C(L = \infty)$ probably would be more accurate. Another method which could have improved this slightly is to average the 5-10 temperatures with the highest C_V. However, this would not necessary give an increase in precision.

References

[1] Morten Hjorth-Jensen. Computational physics: Lecture notes fall 2015. Department of Physics, University of Oslo, 8 2015. Chapter 12 and 13.

[2] Lars Onsager. Crystal statistics. i. a two-dimensional model with an order-disorder transition. *Phys. Rev.*, 65:117–149, Feb 1944.

Appendix

Table 6.1: Alle the microstates of the 2×2 Ising model

State	Spinn	Energi	Magnetization
1	$\downarrow\downarrow$ $\downarrow\downarrow$	$-8J$	-4
2	$\downarrow\downarrow$ $\downarrow\uparrow$	0	-2
3	$\downarrow\downarrow$ $\uparrow\downarrow$	0	-2
4	$\downarrow\uparrow$ $\downarrow\downarrow$	0	-2
5	$\uparrow\downarrow$ $\downarrow\downarrow$	0	-2
6	$\downarrow\downarrow$ $\uparrow\uparrow$	0	0
7	$\downarrow\uparrow$ $\downarrow\uparrow$	0	0
8	$\downarrow\uparrow$ $\uparrow\downarrow$	8J	0
9	$\uparrow\downarrow$ $\downarrow\uparrow$	8J	0
10	$\uparrow\downarrow$ $\uparrow\downarrow$	0	0
11	$\uparrow\uparrow$ $\downarrow\downarrow$	0	0
12	$\downarrow\uparrow$ $\uparrow\uparrow$	0	2
13	$\uparrow\downarrow$ $\uparrow\uparrow$	0	2
14	$\uparrow\uparrow$ $\downarrow\uparrow$	0	2
15	$\uparrow\uparrow$ $\uparrow\downarrow$	0	2
16	$\uparrow\uparrow$ $\uparrow\uparrow$	$-8J$	4